 MCB, vol.2, no.1, pp.41-52, 2005

The Effect of Longitudinal Pre-Stretch and Radial Constraint on the Stress Distribution in the Vessel Wall: A New Hypothesis

Wei Zhang[1,2], **Carly Herrera**[1], **Satya N. Atluri**[1], **Ghassan S. Kassab**[2,3]

Abstract: It is well known that blood vessels shorten axially when excised. This is due to the perivascular tethering constraint by side branches and the existence of pre-stretch of blood vessels at the *in situ* state. Furthermore, vessels are radially constrained to various extents by the surrounding tissues at physiological loading. Our hypothesis is that the axial pre-stretch and radial constraint by the surrounding tissue homogenizes the stress and strain distributions in the vessel wall. A finite element analysis of porcine coronary artery and rabbit thoracic aorta based on measured material properties, geometry, residual strain and physiological loading is used to compute the intramural stresses and strains. We systematically examined the effect of pre-stretch and external radial constraint in both vessels. Our results show that both stretching in the axial direction and compression in the radial direction lead to a more homogeneous strain and stress state in the blood vessel wall. A "uniform biaxial strain" hypothesis is proposed for the blood vessel wall and the ramifications are discussed.

keyword: Blood vessel, remodeling, homogeneous state, mechanical homeostasis.

1 Introduction

Classically, the no-load state (zero transmural pressure) of a blood vessel was thought to be the zero-stress state. A clear consequence of this assumption was a large transmural stress gradient in the vessel wall. The paradigm changed two decades ago when Fung (1983b) and Vaishnav and Vossoughi (1983) independently observed that the geometry of the zero-stress state is an open sector which is very different from the no-load state. The observation was made through a rather simple but elegant experiment. A radial cut of the no-load state caused the ring to spring open into a sector. The finding of circumferential residual stress removed the concept of stress concentration at the inner wall of the vessel in the *in vivo* state (Chuong and Fung, 1986). The implication of the circumferential residual strain was the "uniform stress" hypothesis proposed by Fung (1983b). The uniform stress hypothesis has been used by Takamizawa and Hayashi (1987, 1988) to predict the material constants of a strain energy density function and by others to understand arterial remodeling in response to changes in physical stress and strain (e.g., Rachev, Stergiopulos, Meister, 1996; Taber and Humphrey, 2001).

The existence of pre-stretch and longitudinal tethering was documented much earlier than circumferential residual strain (Fuchs, 1900; Hesses, 1926; Bergel, 1961; Patel and Fry, 1966; Patel and Vaishnav, 1972; McDonald, 1974). Numerous studies have quantified the degree of axial shortening when a blood vessel is excised from the *in situ* condition; i.e., the *in vitro* axial length is significantly shorter than that of the *in situ* condition under zero pressure (see Review in Guo and Kassab, 2003). The axial pre-stretch is typically characterized by the axial stretch ratio, λ_z, which is the ratio of the axial length of the vessel *in situ* to that *in vitro*. The λ_z has been systematically measured along the length of the canine, porcine and mouse aortas (Han and Fung, 1995; Guo and Kassab, 2003). It was found that λ_z increases along the length of the aorta from 1.1 to 1.6 (larger near the common iliac bifurcation). Recently, we have found that the λ_z for the left anterior descending (LAD) artery is about 1.4 (Lu, Yang, Zhao, Gregersen, Kassab, 2003).

We have also recently determined the effect of surrounding tissue on the mechanical properties of blood vessels. We considered an epicardial coronary artery (LAD artery) surrounded by the passive myocardium. The pressure-cross sectional area (CSA) relation was measured for the LAD artery *in situ* and *in vitro* using digital

[1] Department of Mechanical and Aerospace Engineering and
[2] Department of Biomedical Engineering, University of California, Irvine, CA, USA.
[3] Corresponding author. Ph: (949) 824-9490; Fax: (949) 824-9932; E-mail: gkassab@uci.edu.

subtraction angiography (Hamza, Dang, Lu, Mian, Molloi, Kassab, 2003). We found that, at pressure of 100 mmHg, the CSA *in situ* is 34% smaller than that at the *in vitro* state. This corresponds to a 19% decrease in diameter due to the surrounding tissue constraint. Hence, the coronary arteries have axial pre-stretch and are radially constrained by the surrounding tissue and myocardium (Hamza, Dang, Lu, Mian, Molloi, Kassab, 2003). The obvious question is: What are the mechanical implications of these observations?

Although the effect of circumferential residual strain on the *in vivo* intramural stress distribution has been thoroughly investigated (see Review in Rachev and Greenwald, 2003), there are few similar studies on the axial pre-stretch and the external radial constraint by the surrounding tissue. Hence, our objectives are to determine the effect of these factors on the distribution of intramural stresses and strains in the coronary artery wall. Our hypothesis is that the axial pre-stretch and radial constraint by the surrounding tissue homogenizes the circumferential and axial stresses and strains *in vivo*. A finite element method was used to determine the distributions of intramural stresses and strains in the vessel wall under different axial pre-stretch and radial constraints. The results of the study are important since stresses and strains are intimately related to the physiology and patho-physiology of the arterial wall.

2 Model

A finite element method is used to take into account the non-linear constitutive properties of the vessel. A straight, cylindrical vessel is considered with a length $L = 3$ cm (Figure 1). At the no-load state, the inner radius and wall thickness are taken as $r_i = 1.202$ mm and $T = 0.544$ mm, respectively (Kassab, unpublished data for LAD artery). The solid area is discretized into 1500 rectangular elements.

The mechanical behavior of the artery is assumed to obey an exponential-type constitutive model proposed by Fung (Chuong and Fung, 1986):

$$\overline{W} = \frac{c_0}{2}\left\{\exp\left[c_1\overline{E}_r^2 + c_2\overline{E}_z^2 + c_3\overline{E}_\theta^2 + 2(c_4\overline{E}_r\overline{E}_z + c_5\overline{E}_z\overline{E}_\theta + c_6\overline{E}_\theta\overline{E}_r)\right] - 1\right\}, \tag{1}$$

where $\overline{W}$ is the pseudo-strain energy density. $\overline{E}_r$, $\overline{E}_z$ and $\overline{E}_\theta$ denote the scaled Green's strains in the radial, axial and circumferential directions, respectively. The strains are related to the "normalized–stretch-ratios" by

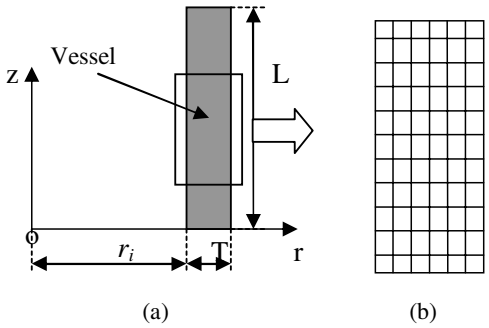

Figure 1 : Schematic of the axisymmetric model (not to scale) and a portion of its finite element mesh.

$$\overline{E}_i = \frac{1}{2}(\overline{\lambda}_i^2 - 1) \quad (i = r, z, \theta) \tag{2}$$

The normalized-stretch-ratios are defined as the corresponding principal stretch ratios (λ_r, λ_z, λ_θ), divided by the cubic root of the third invariant ($J = \lambda_r\lambda_z\lambda_\theta$) of the deformation gradient as per

$$\overline{\lambda}_r = \lambda_r J^{-1/3}, \quad \overline{\lambda}_z = \lambda_z J^{-1/3}, \quad \overline{\lambda}_\theta = \lambda_\theta J^{-1/3}. \tag{3}$$

For large deformations of *isotropic materials*, the Cauchy stress, and its work-conjugate, the Hencky (logarithmic) strain are the proper measures of true stress and strain defined in the deformed configuration (Atluri, 1984). However, the stress-strain relation should be properly established between the second Piola-Kirchhoff stress and the Green-Lagrange strain, for *anisotropic materials* (Atluri, 1984), as shown in Fung's model (Eq. (1)). The derivatives of strain energy are the second Piola-Kirchhoff stresses. The principal logarithmic strains are simply

$$\varepsilon_i = \ln\lambda_i \quad (i = r, z, \theta). \tag{4}$$

If we take into account the incompressibility of the blood vessel by the method of a Lagrangian multiplier, the Cauchy stresses can be expressed as

$$\sigma_{ij} = \frac{\rho}{\rho_0}\frac{\partial x_j}{\partial X_\alpha}\frac{\partial x_i}{\partial X_\beta}\frac{\partial \overline{W}}{\partial E_{\beta\alpha}} + \eta\frac{\partial \varphi}{\partial \varepsilon_{ij}} \quad (i, j, \alpha, \beta = r, z, \theta), \tag{5}$$

where x_i and X_α denote coordinates, and ρ and ρ_0 represent densities, in the deformed and reference states,

respectively. Here, $\varphi(J) = (J-1)^2$ is selected as the penalty function to impose the volume-conserving constraint (Atluri and Reissner, 1989). The parameter η reflects the incompressibility of the material. Note that summation is assumed in Eq. (5) for indexes α and β.

For ideally incompressible materials, J=1 and $\rho = \rho_0$. Hence, the above equations are exactly the same as those presented by Chuong and Fung (1986) or Rachev, Stergiopulos, Meister (1996). The material properties for a representative LAD artery are: $c_0 = 13.7$ kPa, $c_1 = 5.7$, $c_2 = 3.1$, $c_3 = 0.87$, $c_4 = 2.7$, $c_5 = 0.66$, $c_6 = 0.41$ (Kassab, unpublished data). These parameters were obtained by varying the stretch ratio and internal pressure systematically for a coronary arterial segment. The stress-strain relationship was then derived based on the loading and deformation data in reference to the zero-stress state. A relatively large penalty parameter $\eta =$ 1000 kPa is used in our simulations.

The assumption of incompressibility yields the following principal stretch ratios (Rachev, Stergiopulos, Meister, 1996)

$$\lambda_r = \frac{R}{\lambda_z \chi r}, \quad \lambda_z = \frac{z}{Z}, \quad \lambda_\theta = \frac{\chi r}{R}, \tag{6}$$

where R denotes the radius of an arbitrary point at zero-stress state (an open sector), r is the radial coordinate in the deformed configuration, $\chi = \pi/(\pi - \Phi)$ is a factor that depends on the opening angle Φ, which is defined as the angle subtended by two radii connecting the midpoint of the inner wall of the open sector. The inner and outer radii at no-load state and zero-stress state can be obtained as: $r_i = 1.202, r_e = 1.746, R_i = 3.519, R_e = 4.053$ mm, which correspond to $\chi = 2.523$ and an opening angle $\Phi =$ 108.7° when assuming $\lambda_z = 1$ from the zero stress state to the no-load state (Frobert, Gregersen, Bjerre, Bagger, Kassab, 1998). The relationship between the undeformed coordinate and the deformed (no-load) coordinate can be written as (Rachev, Stergiopulos, Meister, 1996)

$$R = \sqrt{\chi(r^2 - r_i^2) + R_i^2}. \tag{7}$$

Equations (4), (6) and (7) can be combined to give the residual strains at the no-load state. To simulate the physiological (*in vivo*) condition, we first stretch the artery from the no-load configuration, and then pressurize the inner vessel surface (e.g., 120 mmHg). To accomplish these tasks, the lower end of the vessel (see Fig. 1) is not allowed to move in the axial direction (the displacement in the axial direction is fixed to zero), and the displacement of the other end along the axial direction is ramped from zero to the desired stretch ratio, and kept constant thereafter. The pressure on the inner surface is then increased linearly from 0 to 16 kPa (120 mmHg), and maintained constant. To investigate the influence of the stretch ratio on stress and strain distributions, the stretch ratio is varied between 1.15 and 1.5. ANSYS Multiphysics (ANSYS, 2003) is selected as the numerical tool. Fung's exponential constitutive model is programmed and linked to ANSYS through the user subroutine USERMAT. In the user subroutine, the geometric dimensions of the blood vessel at zero-stress state and no-load state are used to compute the residual strains. In the subsequent calculations, the zero-stress state is used as the reference state and the total strains, including both the residual strains and the strains accumulated from the no-load state, are used to compute the total stresses.

3 Results

The simulations were performed on a DELL desktop computer running Windows XP Professional. A single Pentium 4 CPU operating at 2.4 GHz and 512 MB of RAM were available on this machine. A typical run for a full analysis takes about 30 minutes.

3.1 Effect of circumferential residual strain

The three components of residual strain are shown in Figure 2(a). Figure 2(b) shows the distributions of circumferential stress in the vessel wall, with and without the circumferential residual strain. It is clearly seen that the residual strain greatly reduces the stress gradient. In all subsequent results, the circumferential residual strain is taken into account.

3.2 Effect of axial pre-stretch

The effect of axial pre-stretch on strain and stress distribution was examined through a series of simulations with $\lambda_z = 1.15, 1.2, 1.3, 1.4$ and 1.5, respectively. Figures 3(a) and (b) show the principal Cauchy stress and logarithmic strain at λ_z = 1.4, respectively. The transmural variations of stress and strain are averaged over the thickness of the wall and are shown in Figures 3(c) and (d), respectively, for various λ_z. The radial stress did not vary with the change in stretch ratio. It is seen that the circumferential

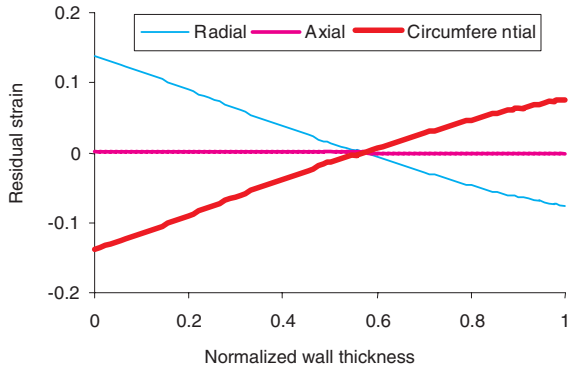

(a)

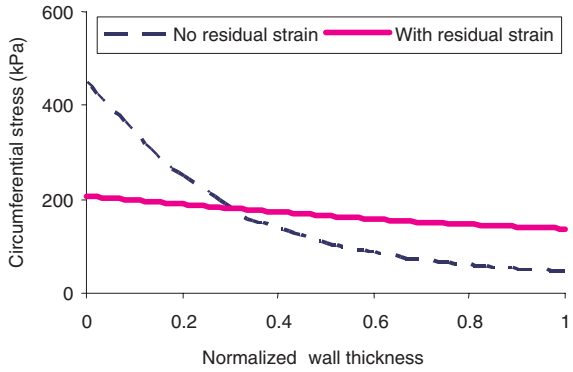

(b)

Figure 2 : (a) Distribution of logarithmic residual strains throughout the wall thickness of the LAD artery. (b) Circumferential Cauchy stress distributions in the vessel wall at physiological conditions (for axial stretch ratio of 1.4 and internal pressure of 120 mmHg) for the porcine LAD artery.

stress and the axial stress both increase with an increase in stretch ratio (Fig. 3(c)). The increase in axial stress, however, is much larger than the circumferential stress. As the λ_z increases, the axial stress gradually reaches the magnitude of circumferential stress. Figure 3(d) reveals that the change of λ_z influences the radial and circumferential strains as well as the axial strain. The radial strain, which is always compressive, becomes more compressive with an increase in λ_z. The axial strain which is completely prescribed by the axial stretch ratio is uniformly distributed in the vessel wall and proportional to λ_z. The circumferential strain, which is dominated by the physiological pressure, appears to be less sensitive to the variation of λ_z.

3.3 *Effect of external constraint*

In the above simulations, we have assumed that there is no constraint on the vessel surface (zero-traction on the outer surface). To gain insight into the effect of radial constraint, we conducted the following simulations. We applied various displacement boundary conditions to constrain the outer surface to different extents, while keeping the internal pressure at 120 mmHg and the stretch ratio at 1.4. These simulations mimic the pressurized *in situ* coronary artery whose outer surface cannot reach the same maximum displacement as that *in vitro* (outer radius of 2.61 mm). Hence, the vessel is compressed by the surrounding myocardium at physiological blood pressure (Hamza, Dang, Lu, Mian, Molloi, Kassab, 2003). Figures 4(a) and (b) show the intramural distribution of stress and strain, respectively, when the outer radius is compressed by 10% (radius of 2.35 mm). It is noted that the effect of radial constraint is to increase the radial stress (see Figure 4(a)) but decrease the tensile axial and circumferential stresses significantly (as compared to Fig. 3(a)). Figure 4(b) shows that the magnitudes of radial and circumferential strains are also decreased as compared to Figure 3(b). The simulation results indicate that the wall stress (especially the circumferential stress, see Fig. 4(a)) can be considerably reduced by an external rigid constraint.

Figures 4(c) and (d) are the average stresses and strains, respectively, at various degrees of radial compression (from 0 to 30%). For the same internal pressure (120 mmHg) and axial stretch ratio (1.4), external compression reduces both the average circumferential and axial stresses. Furthermore, it creates equivalent stresses in the axial and circumferential directions at 8% radial compression in the blood vessel wall (Figure 4(c)). Figure 4(d) shows that the average radial and circumferential strains decrease with the degree of external compression, but the variations of strains are not as large as those of stresses because the material is highly nonlinear. At 15% radial compression, the axial and the circumferential strains become identical. Thus, a bi-axially homogeneous strain state is obtained when the lumen diameter is externally compressed by 15%. At this degree of compression, the corresponding stresses are also nearly homogeneous (Figure 4(c)).

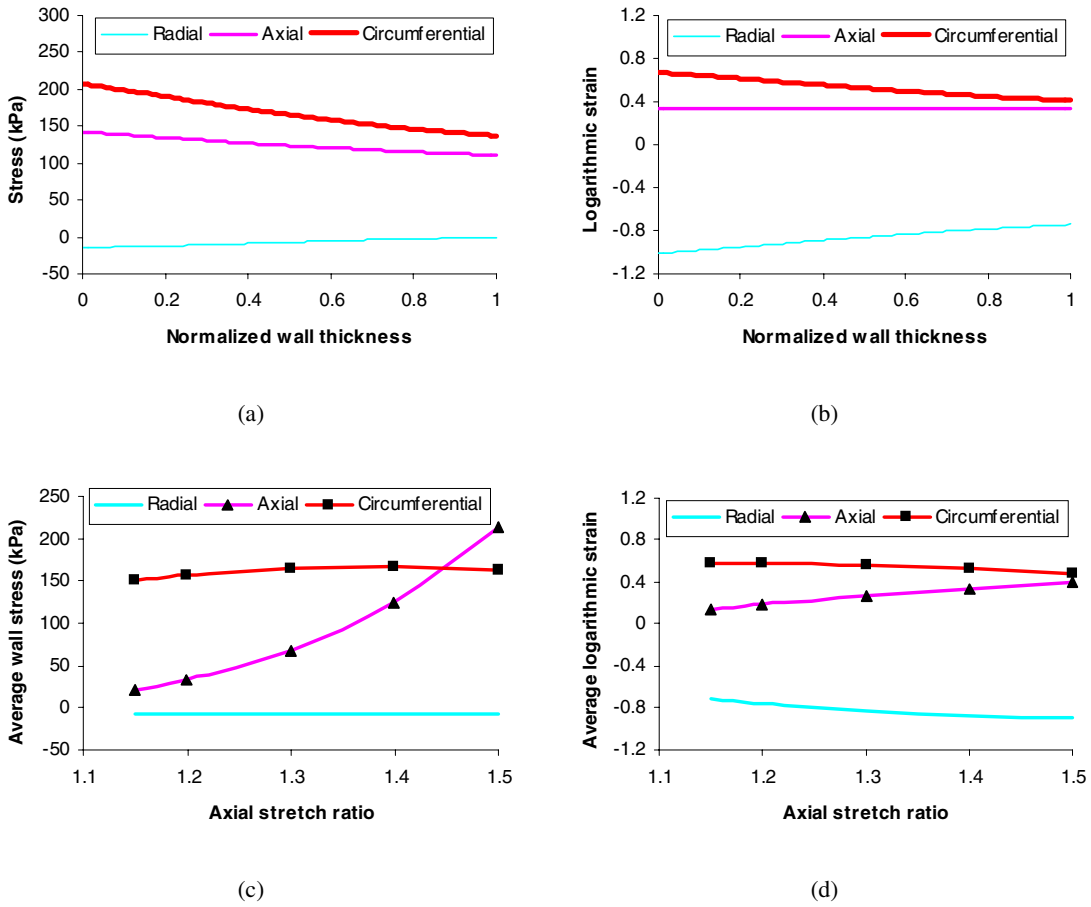

Figure 3 : Distributions of Cauchy stress (a) and logarithmic strain (b) in the vessel wall at the *in vivo* state (axial stretch ratio of 1.4 and internal pressure of 120 mmHg). (c) Average wall stress versus axial stretch ratio. (d) Average wall strain versus axial stretch ratio. The vessel corresponds to the porcine LAD artery.

3.4 Rabbit thoracic aorta

To examine the applicability of our conclusions to other blood vessels, we used another set of material parameters for the rabbit aorta. Chuong and Fung (1986) previously reported the material constants of the rabbit thoracic aorta as: c_0=22.40 kPa, c_1=0.0499, c_2=0.4775, c_3=1.0672, c_4=0.0585, c_5=0.0903, c_6=0.0042. The corresponding dimensions are: R_e=4.52, R_i=3.92, r_e=1.99, r_i=1.39 mm. For an *in vivo* stretch ratio of 1.7 and an internal pressure 120 mmHg, it was found that the axial stress is about one half of the circumferential stress, as shown in Figure 5(a). The circumferential strain is nearly equal to the axial strain (Figure 5(b)). An increase in axial stretch ratio results in larger average circumferential and axial stresses (Figure 5(c)). Similar to the coronary artery, the increase in axial stress is greater than that of the circumferential stress. Figure 5(d) shows that the axial strain is equal to the circumferential strain at the reported *in vivo* stretch ratio of 1.691 (Chuong and Fung, 1986). If a 10% radial compression is assumed (for constant stretch ratio of 1.7), the circumferential and axial stresses decrease to the same level (Figure 5(e)). The strain in the circumferential direction also decreases and becomes smaller than the axial strain (Figure 5(f)).

4 Discussion

4.1 Role of circumferential residual strain

The role of circumferential residual strain has been well studied in the past two decades (see Review in Rachev and Greenwald, 2003). Although the residual stress at no-load state is relatively small in magnitude, it signif-

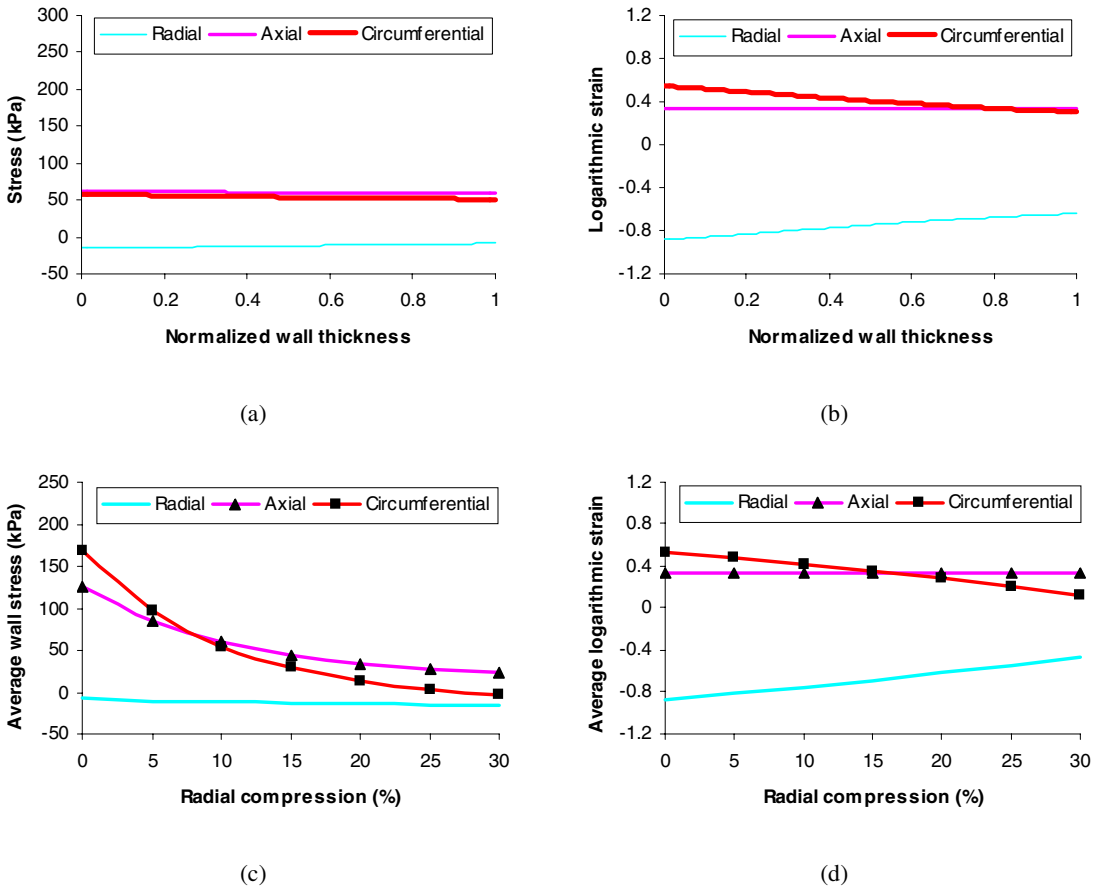

Figure 4 : Stress and strain distributions in vessel wall in the case with radial compression by 10%: (a) stress, (b) strain. (c) Average wall stresses versus radial compression. (d) Average wall strains versus radial compression. The vessel corresponds to the porcine LAD artery.

icantly contributes to the homogeneity of circumferential stress. The compressive and tensile circumferential residual strains on the inner and outer sides of the vessel wall, respectively, compensate the tensile circumferential strain caused by the blood pressure. Hence, there is a significant reduction of stress gradient in the vessel wall (Figure 2(b)) due to the high nonlinearity of the stress-strain relation.

4.2 Role of axial pre-stretch

In vivo, the change in vessel length in the cardiovascular cycle is negligible as compared to the pulsation of diameter. The length is constrained by vessel branches and surrounding tissue. More importantly, the vessel is also pre-stretched longitudinally (Dobrin, Schwarcz, Mrkvicka, 1990). The longitudinal retraction is small in the young and increases with postnatal growth and development as the vessels are stretched by body growth (Dobrin, Canfield, Sinha, 1975). In the present study, we found that an increase in axial stretch tends to increase the axial stress and strain much more significantly than their circumferential counterparts for both the porcine LAD artery and rabbit aorta (Figures 3(c) and 5(c), respectively). For the coronary artery, a stretch ratio of 1.4-1.5 results in identical circumferential and axial stresses and strains. This is interesting since the axial pre-stretch ratio for the LAD artery is about 1.4 (Lu, Yang, Zhao, Gregersen, Kassab, 2003). The foregoing results indicate that the circumferential and axial wall stresses and strains in the LAD artery become more uniform as the axial pre-stretch ratio increases. In other words, under the same physiological pressure, a more homogeneous stress state may be obtained by pre-stretching the vessel. Hence, the axial pre-stretch at the *in vivo* state may play a similar role as the

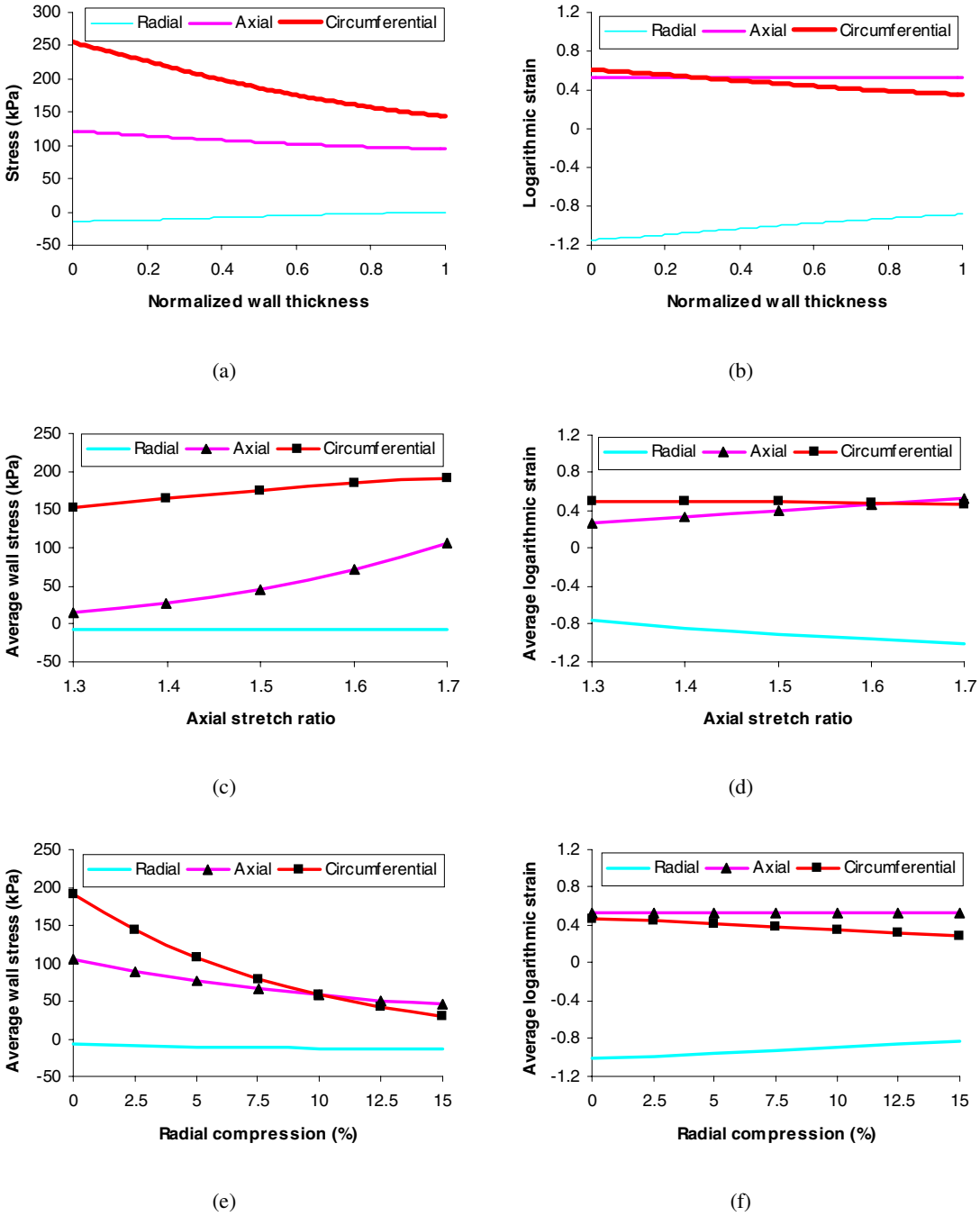

Figure 5 : Stress (a) and strain (b) distributions in a rabbit thoracic artery subjected to stretch ratio 1.7 and pressure 120 mmHg. (c) Average stress and (d) average strain versus prescribed stretch ratio. (e) Average stress and (f) average strain vs. radial compression.

circumferential residual strain does, i.e., makes the stress and strain more homogeneous in the vessel wall. For the aorta, the *in vivo* axial stretch ratio of 1.7 yields similar circumferential and axial strains but not their stress counterparts (Figures 5(c) and (d)).

Our numerical results indicate that the increase of stretch ratio reduces the circumferential strain slightly, which makes the blood vessel "stiffer". This implies that the circumferential strain cannot be effectively decreased by increasing the axial deformation. The observation that axial stretch increases the circumferential stiffness of a blood vessel has been previously confirmed experimentally (Cox, 1975; Vaishnav and Vossoughi, 1983; Weizsacker, Lambert, Pascale, 1983; Dobrin, 1986; Humphrey, Kang, Sakarda, Anjanappa, 1993).

Interestingly, we found that the circumferential stress decreases significantly if the axial stretch ratio is increased when an isotropic Mooney-Rivlin model is used for the vessel wall (results are not shown). This is in sharp contrast to the predictions of the anisotropic model (Figures 3(c) and 5(c)). Thus, it is questionable how well an isotropic model can represent the anisotropic arteries. The increase of stress in Mooney-Rivlin model most likely cannot keep up with the exponential trend found in blood vessels for large strains. Hence, the non-isotropic properties of the vessel wall must be considered in modeling the intramural stress distribution.

4.3 Role of surrounding tissue

All blood vessels receive some perivascular support from the surrounding tissue. Some vessels such as pulmonary arteries receive little support while skeletal, myocardial, or vertebral vessels are much more constrained (see Review in Fung, 1983a). Our analysis shows that even a small external compression (10%) of the LAD artery causes a large reduction in circumferential stress and tends towards a biaxially (circumferential and axial) uniform strain state. For the coronary arteries, it also tends towards a biaxially uniform stress state. In the aorta, a 10% radial constraint results in homogeneity of stresses at the expense of strains (Figure 5(e) and (f)). Hence, it appears that the aorta cannot have simultaneous uniform circumferential and axial stresses and strains, which is in contrast to the coronary artery. Since the geometry, residual strain and physiological loading are similar for the two vessel types, the difference lies in the material properties. We expect that the uniform strain state is more physiological since the thoracic aorta is not as radially compressed as the coronary artery. Guo and Kassab (2003) have found the radial compression to be less than 5% for the mouse thoracic aorta.

In the present simulation, the internal pressure is maintained constant (120 mmHg) while a displacement boundary condition is used to mimic external compression on the artery by the surrounding tissue. The compression is caused by an effective external pressure (external radial stress) which reduces the transmural pressure. Hence, a reduction in transmural pressure decreases the stress concentration. The simulation of displacement is preferred over pressure or radial stress because the change of the latter is less obvious (Figure 4(a)) due to the non-linear material properties of the vessel wall. Furthermore, it is difficult to experimentally determine the stress boundary condition at the adventitia of a coronary artery and hence the transmural pressure is generally unknown whereas accurate measurements of displacement can be made as shown by Hamza, Dang, Lu, Mian, Molloi, Kassab (2003).

The equivalent radial stresses at the external surface of the LAD artery and thoracic aorta can be derived from Figures 4(c) and 5(e), respectively; where the relation between average radial stress and radial compression was plotted. Since the internal pressure is 120 mmHg (16kPa), the radial stress at the inner surface is -16 kPa, the equivalent external pressure P_e is thus calculated by P_e=-(2σ_r+16), where σ_r is the average radial stress. It should be noted that the radial stress is essentially linearly distributed through the thickness of the wall as shown in Figures 3(a), 4(a), and 5(a). The resulting relation between external pressure and radial displacement is shown in Figures 6(a) and (b) for the LAD artery and thoracic aorta, respectively. Additionally, we can express the stresses and strains as a function of transmural pressure as shown in Figures 7(a) and (b) for the LAD artery and 7(c) and (d) for the thoracic aorta. The conclusions are, of course, unchanged.

4.4 Generalization of the uniform strain hypothesis

Takamizawa and Hayashi (1988) proposed a uniform strain hypothesis which states that the circumferential strain is constant across the vessel wall. We agree that the uniform hypothesis should be formulated in terms of strain rather than stress. Strain can be measured directly while stress must be calculated from deformation.

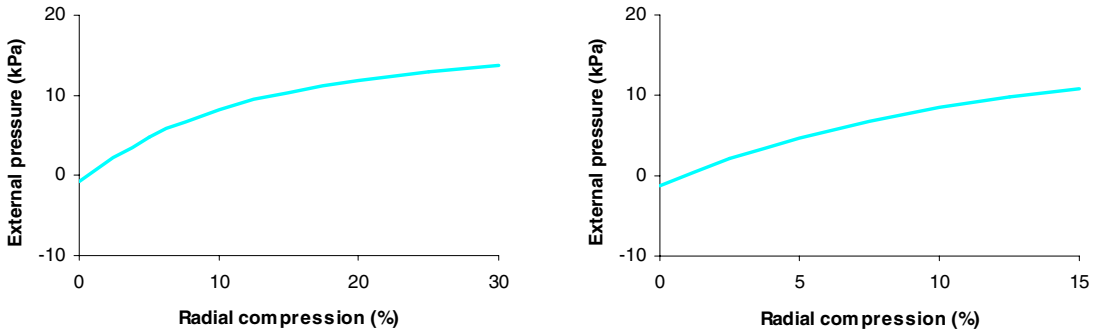

(a) (b)

Figure 6 : The relation between external pressure and radial displacement for (a) the LAD artery and (b) thoracic aorta.

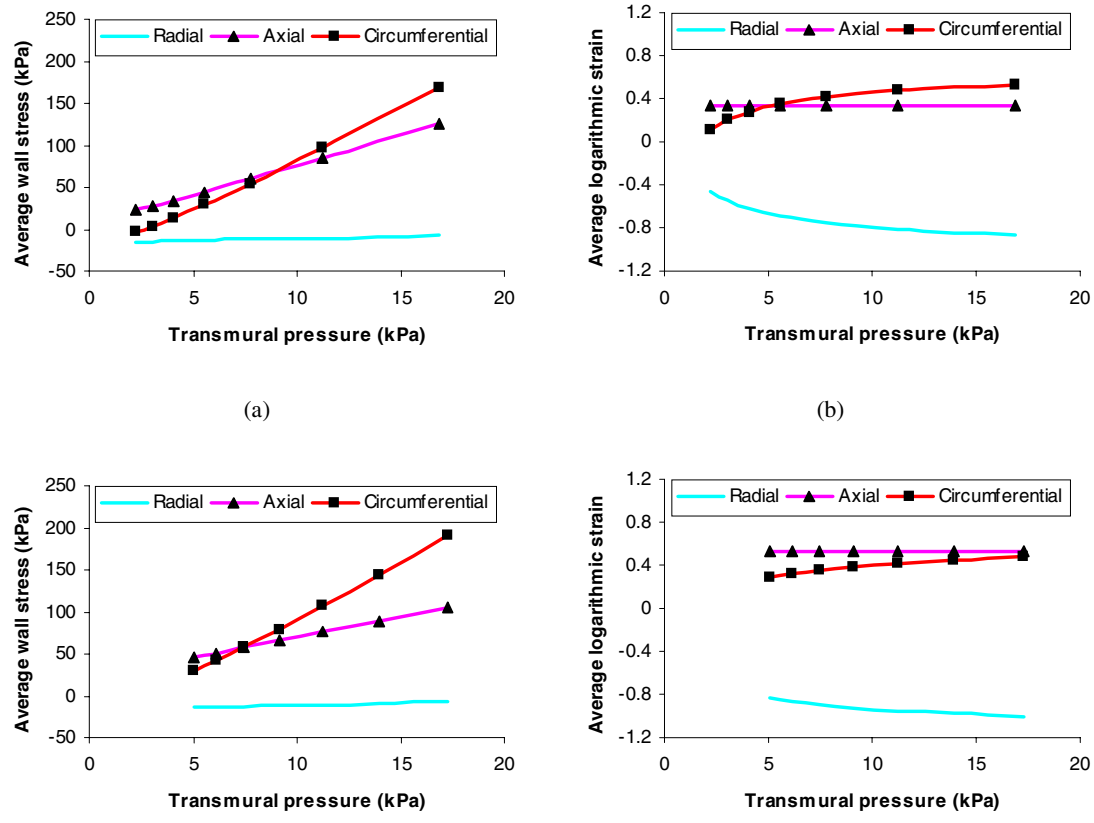

(a) (b)

(c) (d)

Figure 7 : The relation between stress (a and c) and strain (b and d) and the transmural pressure for the LAD artery (a and b) and thoracic aorta (c and d), respectively. The transmural pressure is defined as inner minus outer pressure.

Stress depends on constitutive models and material properties while strain is a more direct concept. Furthermore, the continuity of strain usually introduces a stress discontinuity at the interface of different material layers when a composite model is considered for the blood vessel wall (e.g., Peterson and Okamoto, 2000; Taber and Humphrey, 2001). Based on our simulation results, we propose the generalization of the uniform strain hypothesis to the "uniform biaxial strain" hypothesis. The previous hypothesis relates to transmural uniformity of circumferential strain while the present hypothesis includes the uniformity of circumferential and axial strains at *in vivo* state.

Theoretically, it is impossible to attain uniformity with respect to all three principal deformations. The incompressibility condition requires the product of the three principal stretch ratios to equal unity. Hence, the radial logarithmic strain will always equal the negative of the sum of the values of the logarithmic strains of the other two principal directions. If the circumferential and axial logarithmic strains are equal as postulated by our hypothesis, then the radial logarithmic strain must equal twice the homoeostatic strain. The uniformity of radial strain may not be as important, however, since for a thin walled vessel the effect of radial strain and stress is less significant. Furthermore, the radial stress and strain may be more important for transport of nutrient across the vessel wall but less important as mechano-sensors. The circumferential strain, for example, has a basis as a stimulus for mechano-transduction via activation of ion channels (Sachs, 1988). It would be interesting to investigate a similar role for axial stretch.

4.5 Implications for vessel growth and remodeling

The ability of living tissues to adapt to altered mechanical loading conditions makes them very different from inanimate objects. It has been shown that stress and strain are the major stimuli for growth and remodeling (Kassab, Gregersen, Nielsen, Lu, Tanko, Falk, 2002). For example, arteries change their structures, compositions, and material properties when blood pressure increases (Fung, 1993). The increase in residual strain in blood vessels in response to hypertension has been well documented (see Review in Fung, 1993). It is hypothesized that the increase in opening angle and accompanying residual strain serves to maintain a uniform stress gradient despite the hypertension (Fung and Liu, 1989). Theoretical models have also been developed to account for the stress-dependent adaptation of arteries (e.g., Rachev, Stergiopulos, Meister, 1996; Taber and Humphrey, 2001). These models take into account the circumferential residual strain. We are unaware of any studies that have examined the effect of tissue growth and remodeling on the axial pre-stretch. Conversely, Han, Ku, Vito (2003) examined the effect of axial stretch on vascular cell function and remodeling of blood vessel wall in an ex-vivo system. They concluded that axial stretch promotes cell proliferation in arteries while maintaining arterial function.

4.6 Critique of study

The convergence of the simulation results is verified by the use of a finer finite element mesh. It was found that no significant changes of vessel wall stresses are introduced by imposing four times as many elements (i.e., when element size is reduced to half of the current size).

It was noted in the simulations that for blood vessels with larger opening angles, negative stress gradient can occur (i.e., inner stress is smaller than outer stress). We believe that the implementation of such large bending deformation may lead to numerical errors. It is clear that χ becomes infinite when the opening angle approaches 180^o and equation (6) becomes invalid. Practically speaking, we found that numerical errors occur for opening angles much smaller than that. The opening angles for the coronary arteries have a large variation; i.e., 90-200^o(Frobert, Gregersen, Bjerre, Bagger, Kassab, 1998). In the present study, we only considered vessels with smaller opening angles (108^o). The numerical difficulty will be addressed in future studies so that vessels with larger residual strains can be modeled.

A further consideration is that the opening angle may not be the best measure of residual strains. Li and Hayashi (1996) reported an alternative approach for quantifying the residual strains based on measurement of the edge angle. The authors argued that values of residual strain calculated from measurements of the opening angle may be erroneous if the edge angle is not small (also see Rachev and Greenwald, 2003). Even for large opening angles, if the internal pressure is increased, both the circumferential stress and the circumferential strain must have positive gradients (larger on the inner surface). Therefore, the anisotropy and nonlinearity of the material model must be kept in mind when interpreting stress distributions in

a vessel wall that has large residual strains.

We should remark on the use of logarithmic strains since most biomechanics studies use Green's strains. The logarithmic strain is convenient to check the incompressibility condition which requires that the sum of the three strain components to be zero. The logarithmic strains can be easily converted to stretch ratios (Eq. (4)), Green's strains and engineering strains. A plot of stretch ratios or engineering strains will make the strain gradient in the vessel wall more obvious, but will not change the conclusions.

The current study does not take into account the effect of muscle tone. The *in vivo* and the residual stresses in arteries have been found to be strongly dependent on muscle tone (Matsumoto, Tsuchida, Sato, 1996; Rachev and Hayashi, 1999). Although the present results are purely of a passive model, they provide the framework for exploring the effect of active contraction in future studies.

Finally, it is well known that soft-tissue models have limitations in that the model can behave very differently depending on the material constants used. Hence, it is important to show that the homogenization of the stress or strain in the vessel wall observed in the present study is not merely model-dependent. In addition to the segments of swine LAD artery and rabbit thoracic aorta, we studied three additional swine coronary arteries from different animals. The conclusion regarding the uniform biaxial stress and strain for the coronary artery under physiological conditions remained unchanged. Other mathematical forms of the strain-energy density function should be examined in future studies.

5 Summary

Stress and strain are intimately related to tissue function, growth and remodeling. Hence, a thorough understanding of the stress and strain state in the normal vessel wall can be used as a physiological reference state. The present simulation reveals that distributions of stresses and strains become more uniform when the axial prestretch is considered and the outer surface is compressed by the surrounding tissues. Hence, at the *in vivo* condition, residual strains in the circumferential, axial and radial directions and surrounding tissue all help to maintain biaxial strain homogeneity or uniformity in the vessel wall. This state may define the mechanical homeostasis of the vessel wall. Initiation of atherosclerosis or other vascular dysfunctions may be caused by perturbations of the homeostatic state of stress and strain. We propose that the physical principle that dictates the growth and remodeling of the vessel wall is to restore the homeostatic biaxial strain state. An experimental test of this hypothesis remains a task of future investigations.

Acknowledgments: We wish to thank Mr. Chong Wang for conducting some of the simulations. This research was supported in part by the National Institute of Health-National Heart, Lung, and Blood Institute Grant 5 R29 HL55554 and the US Army Research Office. Dr. Kassab is the recipient of the American Heart Association Established Investigator Award.

References

ANSYS (2003): ANSYS 8.0 Online Documentation. ANSYS Inc., http://www.ansys.com.

Atluri, S.N. (1984): Alternate stress and conjugate strain measures, and mixed variational formulations involving rigid rotations, for computational analyses of finitely deformed plates and shells: Part-I: Theory. *Computers & Structures* 18(1): 93-116.

Atluri, S.N.; Reissner, E. (1989): On the formulation of variational theorems involving volume constraints. *Comput Mech* 5(5): 337-44.

Bergel, D.H. (1961): The static elastic properties of the arterial wall. *J Physiol* 156: 445-57.

Chuong, C.J.; Fung, Y.C. (1986): On residual-stresses in arteries. *J Biomech Eng* 108(2): 189-92.

Cox, R.H. (1975): Anisotropic properties of the canine carotid-artery in vitro. *J Biomech* 8(5): 293-300.

Dobrin, P.B. (1986): Biaxial anisotropy of dog carotid-artery: estimation of circumferential elastic modulus. *J Biomech* 19(5): 351-8.

Dobrin, P.B.; Canfield, T.; Sinha, S. (1975): Development of longitudinal retraction of carotid arteries in neonatal dogs. *Experientia* 31: 1295-6.

Dobrin, P.B.; Schwarcz, T.H.; Mrkvicka, R. (1990): Longitudinal retractive force in pressurized dog and human arteries. . *Surg Res* 48: 116-20.

Frobert, O.; Gregersen, H.; Bjerre, J.; Bagger, J.P.; Kassab, G.S. (1998): Relation between the zero-stress state and the branching orders of the porcine left coronary arterial tree. *Am J Physiol* 275 (Heart Circ. Physiol. 44): H2283-90.

Fuchs, R.F. (1900): Zur Physiologie und Wachstummsme-chanik des blutgefassystems. *Arch Ges Physiol* 28: 7.

Fung, Y.C. (1983a): Biodynamics: Circulation. Springer-Verlag, New York.

Fung, Y.C. (1983b): What principle governs the stress distribution in living organisms? In: Fung, Y. C., Fukada, E., Wang. J. J. (Eds.), Biomechanics in China, Japan, and USA. Science Press, Beijing, pp. 1–13.

Fung, Y.C. (1993): Biomechanics: Motion, Flow, Stress and Growth. Springer-Verlag, New York.

Fung, Y.C.; Liu, S.Q. (1989): Change of residual strains in arteries due to hypertrophy caused by aortic constriction. *Circ Res* 65(5): 1340-9.

Guo, X.; Kassab, G.S. (2003): Variation of mechanical properties along the length of the aorta in C57bl/6 mice. *Am J Physiol-Heart Circ Physiol* 285: H2614–22.

Hamza, L.H.; Dang, Q.; Lu, X.; Mian, A.; Molloi, S.; Kassab, G.S. (2003): Effect of passive myocardium on the compliance of porcine coronary arteries. *Am J Physiol-Heart Circ Physiol* 285(2): H653-60.

Han H.C.; Fung Y.C. (1995): Longitudinal strain of canine and porcine aortas. *J Biomech* 28(5): 637-41.

Han, H.C.; Ku, D.N.; Vito, R.P. (2003): Arterial wall adaptation under elevated longitudinal stretch in organ culture. *Ann Biomed Eng* 31(4): 403-11.

Hesses, M. (1926): Uber die pathologischen Veranderungen der Arterien der oberen extremitat. *Virchows Arch Path Anat Physiol* 261: 225-52.

Humphrey, J.D.; Kang, T.; Sakarda, P.; Anjanappa, M. (1993): Computer-aided vascular experimentation: a new electromechanical test system. *Ann Biomed Eng* 21(1): 33-43.

Kassab, G.S.; Gregersen, H.; Nielsen, S.L.; Lu, X.; Tanko, L.B.; Falk, E. (2002): Remodeling of the left anterior descending artery in a porcine model of supravalvular aortic stenosis. *J Hypertension* 20(12): 2429-37.

Li, X.; Hayashi, K. (1996): Alternate method for the analysis of residual strain in the arterial wall. *Biorheology* 33(6): 439–49.

Lu, X.; Yang, J.; Zhao, J.B.; Gregersen, H.; Kassab, G.S. (2003): Shear modulus of coronary arteries: Contribution of media and adventitia. *Am J Physiol-Heart Circ Physiol* 285: H1966-75.

Matsumoto, T.; Tsuchida, M.; Sato, M. (1996): Change in intramural strain distribution in rat aorta due to smooth muscle contraction and relaxation. *Am J Physiol-Heart Circ Physiol* 271(4): H1711-6.

McDonald, D.A. (1974): Blood flow in arteries. William Wilkins, Baltimore.

Patel, D.J.; Fry, D.L. (1966): Longitudinal tethering of arteries in dogs. *Circ Res* 19: 1011-21.

Patel, D.J.; Vaishnav, R.N. (1972): The rheology of large blood vessels. In Cardiovascular Fluid Dynamics (Edited by Bergel, DH), Vol. 2, pp. 1-64. Academic Press, New York.

Peterson, S.J.; Okamoto, R.J. (2000): Effect of residual stress and heterogeneity on circumferential stress in the arterial wall. *J Biomech Eng* 122(4): 454-6.

Rachev, A.; Greenwald, S.E. (2003): Residual strains in conduit arteries. *J Biomech* 36(5): 661-70.

Rachev, A.; Hayashi K. (1999): Theoretical study of the effects of vascular smooth muscle contraction on strain and stress distributions in arteries. *Ann Biomed Eng* 27(4): 459-68.

Rachev, A.; Stergiopulos, N.; Meister, J.J. (1996): Theoretical study of dynamics of arterial wall remodeling in response to changes in blood pressure. *J Biomech* 29(5): 635-42.

Sachs, F. (1988): Mechanical transduction in biological systems. *CRC Crit Rev Biomed Eng* 16(2): 141-69.

Taber, L.A.; Humphrey, J.D. (2001): Stress-modulated growth, residual stress, and vascular heterogeneity. *J Biomech Eng* 123(6): 528-35.

Takamizawa, K.; Hayashi, K. (1987): Strain-energy density-function and uniform strain hypothesis for arterial mechanics. *J Biomech* 20(1): 7-17.

Takamizawa, K.; Hayashi, K. (1988): Uniform strain hypothesis and thin-walled theory in arterial mechanics *Biorheology* 25(3): 555-65.

Vaishnav, R.N.; Vossoughi, J. (1983): Estimation of residual strains in aortic segments. In: C.W. Hall (Ed.), Biomedical Engineering II, Recent Developments, Vol. 2. New York, Pergamon Press, Oxford, pp. 330–3.

Weizsacker, H.W.; Lambert, H.; Pascale, K. (1983): Analysis of the passive mechanical properties of rat carotid arteries. *J Biomech* 16: 703-15.